

Band Structure Effects in Ejection of Ni Atoms in Fine Structure States

C. He,* Z. Postawa,† S. W. Rosencrance, R. Chatterjee, B. J. Garrison, and N. Winograd

Department of Chemistry, 152 Davey Laboratory, The Pennsylvania State University, University Park, Pennsylvania 16802

(Received 22 May 1995)

Kinetic energy distributions of Ni atoms in six electronic fine structure states ejected from a single crystal Ni{001} surface due to bombardment with 5 keV Ar⁺ ions have been measured. These states arise from two different electronic configurations, $3d^84s^2 \{a^3F_{4,3,2}\}$ and $3d^94s^1 \{a^3D_{3,2}$ or $a^1D_2\}$, which form three distinct fine structure manifolds within 0.422 eV of the 3F_4 ground state. We find that the band structure effects dominate leading to larger populations in the excited $^3D_{3,2}$ states than found for the ground state.

PACS numbers: 79.20.Rf, 32.80.Fb, 61.80.Mk

The formation of excited atomic electronic states subsequent to keV ion bombardment of metals has been a research focus for nearly three decades in order to establish the role of inelastic energy transfer in electronic device fabrication and to further the basic understanding of ion-solid interactions. The consensus resulting from quantum-state specific kinetic energy distribution measurements of sputtered particles is that the final population of metastable excited states is dominated by nonradiative deexcitation events that depend largely on the magnitude of the energy gap between the ground and excited state [1]. More recently, experiments with ion-bombarded In [2] and Rh [3] metal, using multiphoton ionization (MPI) for detection of quantum-specific excitations, suggest that the character of the electronic state is at least as important as the magnitude of the energy gap in determining the nonradiative relaxation rate and hence the final population.

In this Letter we report on a systematic study of the energy distributions and populations of Ni atoms ejected from an ion-bombarded Ni{001} crystal. This system possesses the essential attributes necessary to disentangle the influence of the magnitude of the excitation energy from the electronic state character on the final populations since there are two distinct electronic configurations $3d^84s^2 \{a^3F_{4,3,2}\}$ and $3d^94s^1 \{a^3D_{3,2,1}$ and $a^1D_2\}$ that have closely spaced and intertwined energy levels [4]. In contrast to previous studies [5] of metastable states of Ni, our results show for the first time that the peak position of the kinetic energy distribution depends solely on the electronic structure of the sputtered atom. Moreover, the populations exhibit a remarkable behavior in that the excited $^3D_{3,2}$ states are more heavily populated than the ground 3F_4 state, a result consistent with the *D*-like character of the Ni band structure. Hence a simple nonradiative energy transfer theory is inadequate to entirely understand excited state populations and energy distributions during desorption.

The experimental system and the procedure for relating energy distributions to time-of-flight distributions have been described in detail elsewhere [6]. Briefly, the mea-

surements were performed in an ultrahigh vacuum chamber (1×10^{-10} torr base pressure) equipped with low energy electron diffraction (LEED) and Auger spectroscopy. The Ni{001} crystal was cleaned in the traditional fashion by cycles of ion bombardment, oxidation, and thermal annealing until a sharp (1×1) LEED pattern representative of the {001} plane was obtained [7].

To initiate an event, a 250 ns pulse of 6×10^{-6} A 5 keV Ar⁺ ions was focused, at normal incidence, onto a 2 mm spot on the sample. Upon impact of the ion pulse, an extraction field was activated to reject charged sputtered particles. A 6 ns laser pulse with a variable power of 0.1–6 mJ and a cross section of 1 mm \times 10 mm was positioned 1.5 cm above the impact region with a 45° angle between the sample surface and the ribbon-shaped laser beam.

Excited Ni atoms desorb in straight trajectories requiring a few microseconds to reach the photon field. All of the electronic states of interest in this work are metastable with respect to decay to lower states and are hence representative of the population of these states at the instant they are beyond interaction range of the crystal surface. Moreover, cascading from higher levels to those of the *F* and *D* manifolds is not considered significant for clean Ni due to the low initial population of states outside of these manifolds, which lie more than 1.5 eV above the ground state.

Photoionization was achieved using a tunable UV dye laser pumped by a Spectra Physics GCR5 Nd-YAG laser operated at a repetition rate of 30 Hz. Wavelengths from 300 to 305 nm were generated using R640, and wavelengths between 310 and 325 nm were generated using DCM. This laser was employed to selectively ionize a portion of the ejected neutral atoms in a specific quantum state at a delay time τ_E after the ion-pulse impact, thus defining the time of flight. The ionized particles were then accelerated by the extraction field so as to arrive at the front of a microchannel plate detector at time τ_M , which is governed by the mass-to-charge ratio and the initial speed of the ion. By variation of τ_E , it is possible to determine the kinetic energy distribution,

angular distribution, and relative intensity of the ejected Ni atoms in each specified quantum state. Particles were collected between polar angles of 0° and 90° along the <001> azimuth. The Jacobian of transformation to energy distributions has been reported [6].

Ionization of Ni atoms was achieved using the excitation schemes shown in Fig. 1. Although there are many intermediate levels and ionization pathways that could have been chosen for these experiments, our results were obtained using two-photon ionization via the $y^3F_3^0$ level of the $y^3F_J^0$ manifold. This manifold is preferred over the $y^3D_J^0$ manifold since the transition probability for the $y^3F_3^0$ resonant absorption steps are higher than for the y^3D_J steps, and there is negligible interference from Ni⁺ ions produced by photodissociation of Ni₂. The $y^1D_2^0$ intermediate state was selected for photoionization from the 1D_2 level since this scheme most conveniently overlapped the wavelength range of the dye laser. Kinetic energy distributions were obtained from 90 values of τ_E , with each point resulting from the sum of 30 laser shots. Thirty sets of τ_E 's were averaged to create the final energy distributions.

It is more difficult to extract accurate information about the population of a specific quantum state since the cross sections for all the excitation and ionization steps are not known and are not easily determined. To account for possible variations in cross sections, we have compared the

relative intensities found for sputtered Ni atoms to those obtained from thermally evaporated Ni atoms. These experiments were performed by heating a 1 mm Ni wire to 1230 K at 10⁻⁸ torr to a density of 10⁷ Ni atoms/cm³ (10³ Ni₂ molecules/cm³) and ionizing the evaporating species at a distance of 1 mm above the wire [8]. The uncorrected intensities from both experiments are shown in Table I. As a first approximation, deviations from Boltzmann behavior in the evaporation experiment are assumed to arise from cross-section variations. Using this assumption for the cross sections, the correct sputter intensities are given in the final column of Table I. The most striking result is that there are more atoms ejected in the excited 3D_3 and 3D_2 states than in the ground 3F_4 state. As far as we know a population inversion of this sort has not been previously observed during any desorption process.

The population of the states in each manifold with the exception of 3D_2 decreases as the energy above the respective ground state increases in accord with previous observations. Although the data are somewhat scattered, it is possible to fit these populations by a Boltzmann distribution to determine an effective electronic temperature. As a result of this fit, we find that the effective electronic temperature of the *F* manifold is 10 500 ± 800 K, and the effective electronic temperature of the *D* manifold is 810 ± 70 K. The temperature of the *F* manifold is an order of magnitude larger than that found on other systems such as Fe (~600 K) [9], Zr (~800 K) [10], Ti (~300 K) [11], U (~900 K) [12], and Fe from stainless steel (~980 K) [13], whereas the effective temperature of the *D* manifold is comparable to other values. The generality of this observation is not yet known since there are no previous studies that have probed several states within each of two different manifolds.

The measured kinetic energy distributions for sputtered Ni atoms in different quantum states are shown in Fig. 2. These striking results clearly show that the distributions,

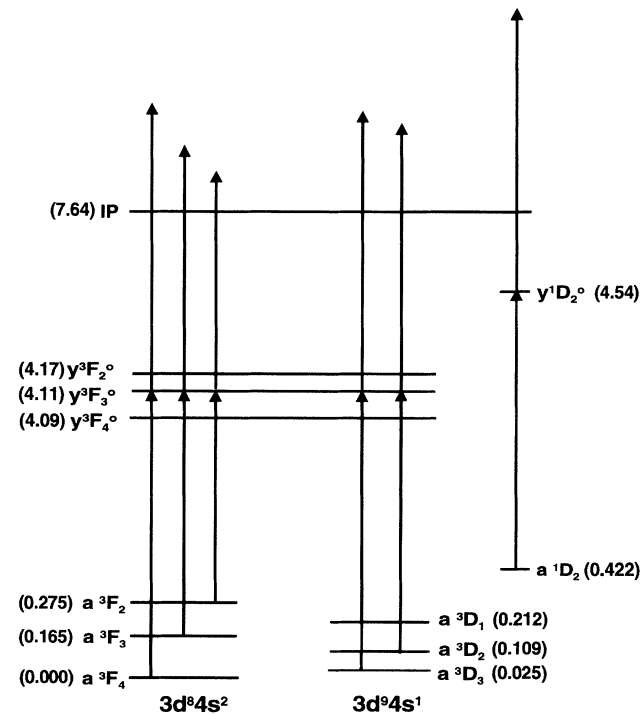


FIG. 1. Partial electronic structure of atomic Ni showing the ionization schemes examined in this work. The energy of each state above the ground state is noted in units of electron volts [4].

TABLE I. Ni energy levels and measured populations.

State	Atomic Config.	Energy (eV) ^a	Intensity ^b	Evaporated intensity ^c	Corrected intensity ^d
3F_4	$3d^8 4s^2$	0.0	1	1	1
3D_3	$3d^9 4s^1$	0.025	4.5	0.62	5.7
3D_2	$3d^9 4s^1$	0.109	520	25	7.4
3F_3	$3d^8 4s^2$	0.165	3	0.66	0.9
3D_1	$3d^9 4s^1$	0.212	0.4	0.16	0.3
3F_2	$3d^8 4s^2$	0.275	15	1.7	0.6
1D_2	$3d^9 4s^1$	0.422	0.89	0.22	0.075

^aFrom Ref. [4].

^bRaw measured intensities from the bombardment experiment.

^cRaw measured intensities from the evaporation experiment.

^dRatio of the bombardment yield to the evaporation yield normalized to a Boltzmann distribution at 1230 K.

Effects of spectroscopic degeneracies and lifetimes are included in these values.

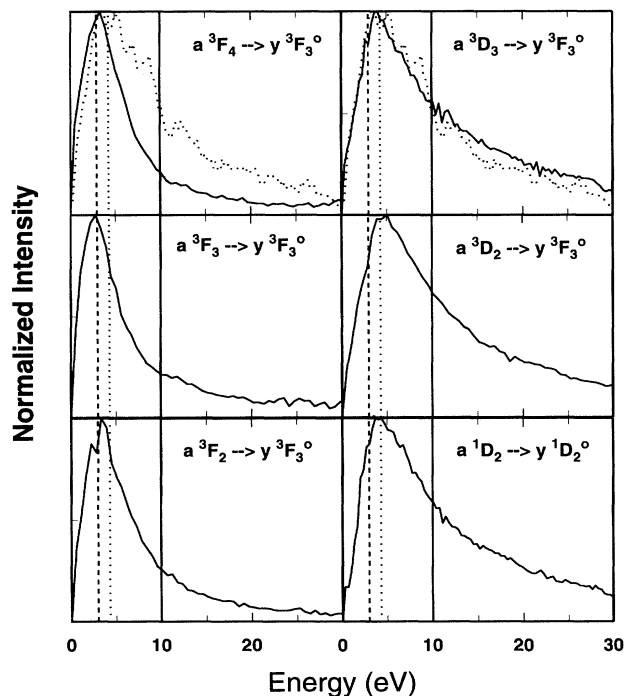


FIG. 2. State-selected angle-integrated kinetic energy distributions of Ni atoms ejected from Ni{001} bombarded with 5 keV Ar⁺ ions. The peak energy of the F states is $\sim 3 \pm 0.5$ eV (dashed vertical line) and the D states peak $\sim 4.3 \pm 0.5$ eV (second dotted vertical line). The intensity at 10 eV divided by the peak intensity is 0.23 ± 0.02 for the F states and is 0.57 ± 0.02 for the D states. The kinetic energy distribution for the 3D_1 state (not shown) is similar to the other D states, although the signal-to-noise ratio of the data is significantly less. The energy distributions denoted by dotted curves drawn with the 3F_4 and 3D_3 distributions are from molecular dynamics simulations [14].

although similar in shape to that predicted by Thompson many years ago [15], fall into two distinct categories. Those atoms originating from the a^3F_J ground state manifold are virtually identical in shape to each other and exhibit a peak at an energy of 3 ± 0.5 eV. Those atoms originating from the a^3D_J and a^1D_2 manifolds are also similar in shape to each other but exhibit a peak at an energy of 4.3 ± 0.5 eV. Hence, for ion-bombarded Ni{001}, the peak position of the kinetic energy distributions depends only on the electronic character of the state and not on the magnitude of the excitation energy required to populate that level. For example, the energy distribution of the 1D_2 state is similar to the 3D_3 state, even though these states are separated by 0.422 eV. Moreover, the 3D_3 state yields a very different kinetic energy distribution than the 3F_4 state, even though they are only separated by 0.025 eV.

The results presented here generally conflict with existing ideas about excited state formation and deexcitation during sputtering. For example, variations in the veloc-

ity distribution have been explained using a nonradiative deexcitation model developed originally for ion scattering and ion neutralization [16]. This model assumes that the rate of deexcitation depends exponentially on the inverse of the magnitude of the velocity component perpendicular to the surface. Hence, the excited state kinetic energy distributions should appear to be broader and peak at a higher value than those for the ground state distribution.

A second model presented more recently by Craig *et al.* [2] suggests that the electronic structure of the fine structure state is the main factor in determining whether a given state will relax. According to this model, for manifolds with a closed outer shell of electrons, the deexcitation rate should be lower than for a manifold that is partially filled due to shielding of the interaction of the departing atom with the metallic band. For Ni, this model is partially successful since the energy distributions of the F manifold, which has a full s shell ($4s^2$), are similar to each other and the energy distributions of the excited D manifold, which has a partially filled s shell ($4s^1$), is broader than the ground 3F_4 state. The broadening has been considered a signature for the presence of more efficient deexcitation to a lower level. These observations were also noted for Fe [10] and Zr [9] excited states with closed outer shells and for Fe [17], Ba [18], Ca [19], and Ti [20] with partially filled outer shells.

A problem arises, however, when examining the populations of each of the Ni electronic states. As noted above, two of the D states are observed to survive with higher probability than the ground 3F_4 state. If these states are more effectively deexcited, presumably back to the atomic configurations of lowest energy, their population would most likely be lower than that found for the ground 3F_4 level. Moreover, deexcitation events within manifolds of similar character must lead to significant differences in observed velocity distributions, differences not evident from the data shown in Fig. 2. Hence, other factors are clearly responsible for the behavior of excited state energy distributions in Ni.

Consideration of the initial electronic configuration of Ni metal allows all of these conflicting observations to be qualitatively reconciled. A variety of spectroscopic measurements and calculations suggest that the d band of Ni has more than nine electrons with one calculation [21] suggesting a configuration of approximately $3d^{9.4}4s^{0.6}$. This electronic structure is much closer to the $3d^94s^1$ character of the ${}^{1,3}D_J$ manifolds of atomic Ni than the 3F_4 manifold. Hence, the observed enhanced D state intensity is a direct consequence of being the predominate bonding state of the metal. This idea is further supported by the shape of the energy distributions themselves. Molecular dynamics simulations [14] using a recently developed molecular dynamics Monte Carlo corrected effective medium many-body potential energy function [22] fit to the bulk cohesive energy for Ni yield energy distributions that match only those observed for the D

manifold as noted in Fig. 2. The shapes of the velocity distributions for F manifold states are characteristic of a solid whose cohesive energy is much less than the 4.46 eV of Ni metal [23]. This result is expected since Ni atoms of F character formed in the collision cascade are much less tightly bound to the solid due to the full nonreactive s shell ($4s^2$).

There are parallels between this picture and the description of the bonding of the Ni_2 dimer. Calculations [24–27] and experiment [28] demonstrate that the ground state of Ni_2 arises from two atoms in the 3D manifold. The interaction of two Ni atoms in F states is purely repulsive [24]. Because of the large number of spin-orbit states [24,27,28], there is considerable mixing of configurations as the atoms separate. Curve crossings in this region, thus, could give rise to the formation of atoms in the F states.

The proposal that the band structure of Ni influences the intensity of sputtered metastable states might also extend to the intensities in the evaporation experiment. If Ni atoms in the 3D manifold evaporate more than 3F Ni atoms, the sputter intensities would exhibit even more enhancement of Ni atoms in the 3D manifold, especially the 3D_2 state.

In summary, we have reported the first study of the energy distributions of atoms sputtered in several excited states from two different electronic manifolds. For Ni, the results support an excitation model whereby the excitation probabilities are dominated by the nature of the band structure of the metal and by the electronic state of the departing atom. Other elements that intertwined energy levels in two fine structure manifolds are W, Os, and Ir [4]. These metals would be interesting test cases for the ideas presented here.

This work was supported in part by grants from the Office of Naval Research, the National Science Foundation, and the M. Curie-Sklodowska Fund No. MEN/NSF-93-144. The authors acknowledge valuable discussions with Robert Bernheim, Terry Miller, Michael Morse, David Shirley, Roy Willis, and Ming Yu.

*Permanent address: SRI International, 333 Ravenswood Ave., Menlo Park, CA 94025.

†Permanent address: Jagellonian University, 30-059 Krakow 16, Reymonta 4, Poland.

[1] M.L. Yu, in *Sputtering by Particle Bombardment III*, edited by R. Behrisch and K. Wittmaack (Springer-Verlag, Berlin, 1991), Chap. 3.

- [2] B.I. Craig, J.P. Baxter, J. Singh, G.A. Schick, P.H. Kobrin, B.J. Garrison, and N. Winograd, *Phys. Rev. Lett.* **57**, 1351 (1986).
- [3] D.N. Bernardo, M. El-Maazawi, R. Maboudian, Z. Postawa, N. Winograd, and B.J. Garrison, *J. Chem. Phys.* **97**, 3846 (1992); **100**, 8557(E) (1994).
- [4] C.E. Moore, *Atomic Energy Levels* (U.S. Government Printing Office, National Bureau of Standards, Washington, D.C., 1971), Vol. 3.
- [5] G. Nicolussi, W. Husinsky, D. Gruber, and G. Betz, *Phys. Rev. B* **51**, 8779 (1995).
- [6] P.H. Kobrin, G.A. Schick, J.P. Baxter, and N. Winograd, *Rev. Sci. Instrum.* **57**, 1354 (1986).
- [7] C. Xu, J.S. Burnham, S.H. Goss, K. Caffey, and N. Winograd, *Phys. Rev. B* **49**, 4842 (1994).
- [8] For a description of this procedure, see J.D. Fassett, L.T. Moore, J.C. Travis, and F.E. Lytle, *Int. J. Mass Spectrom. Ion Phys.* **54**, 201 (1983).
- [9] M.J. Pellin, R.B. Wright, and D.M. Gruen, *J. Chem. Phys.* **74**, 6448 (1981).
- [10] C.E. Young, W.F. Callaway, M.J. Pellin, and D.M. Gruen, *J. Vac. Sci. Technol. A* **2**, 693 (1984).
- [11] M.J. Pellin, C.E. Young, M.H. Mendelsohn, D.M. Gruen, R.B. Wright, and A.B. Dewald, *J. Nucl. Mater.* **111/112**, 738 (1980).
- [12] R.B. Wright, M.J. Pellin, D.M. Gruen, and C.E. Young, *Nucl. Instrum. Methods* **170**, 295 (1980).
- [13] B. Schweer and H.L. Bay, *Vide Couches Minces* **201**, 1349 (1980).
- [14] S.W. Rosencrance, J.S. Burnham, D.E. Sanders, C. He, B.J. Garrison, N. Winograd, and A.E. DePristo, *Phys. Rev. B* **52**, 6006 (1995).
- [15] M.W. Thompson, *Philos. Mag.* **18**, 377 (1968).
- [16] H.D. Hagstrum, *Phys. Rev.* **96**, 336 (1954).
- [17] B. Schweer and H.L. Bay, *Appl. Phys. A* **29**, 53 (1982).
- [18] M.L. Yu, D. Grischkowsky, and A.C. Balant, *Phys. Rev. Lett.* **48**, 427 (1982).
- [19] W. Husinsky, G. Betz, and I. Girgis, *Phys. Rev. Lett.* **50**, 1689 (1983).
- [20] E. Dullni, *Appl. Phys. A* **38**, 131 (1985).
- [21] J.W.D. Connolly, *Phys. Rev.* **159**, 415 (1967).
- [22] T.J. Raeker and A.E. DePristo, *Int. Rev. Phys. Chem.* **10**, 1 (1991).
- [23] *CRC Handbook*, edited by R.C. Weast (CRC Press, Inc., Boca Raton, 1981/1982), 62nd ed., p. F190.
- [24] I. Shim, J.P. Dahl, and H. Johansen, *Int. J. Quantum Chem.* **15**, 311 (1979).
- [25] T.H. Upton and W.A. Goddard III, *J. Am. Chem. Soc.* **100**, 5659 (1978).
- [26] J.O. Noell, M.D. Newton, P.J. Hay, R.L. Martin, and F.W. Bobrowicz, *J. Chem. Phys.* **73**, 2360 (1980).
- [27] E.M. Spain and M.D. Morse, *J. Chem. Phys.* **97**, 4641 (1992).
- [28] J.C. Pinegar, J.D. Langenberg, C.A. Arrington, E.M. Spain, and M.D. Morse, *J. Chem. Phys.* **102**, 666 (1995).